

# LMDZ physical schemes. A brief description for the LMDZ-B configuration

L. Fita

Laboratoire de Météorologie Dynamique, IPSL, UPMC, CNRS, Tw. 45-55 3rd fl., B99, Jussieu, 75005, Paris, France

August 22, 2013

## Contents

<b>1</b>	<b>Introduction</b>	<b>2</b>
<b>2</b>	<b>Radiation scheme</b>	<b>2</b>
<b>3</b>	<b>PBL, convection and cumulus schemes</b>	<b>3</b>
3.1	Planetary Boundary Layer scheme . . . . .	5
3.1.1	Thermal . . . . .	5
3.1.2	Cold pools . . . . .	6
3.2	Deep convection . . . . .	7
3.3	Cumulus scheme . . . . .	8
<b>4</b>	<b>Micro-Physics scheme</b>	<b>9</b>
<b>5</b>	<b>Land scheme</b>	<b>9</b>
5.1	SVAT SECHIBA . . . . .	10
5.1.1	Bulk aerodynamic method . . . . .	12
5.2	Orchidee . . . . .	13
<b>6</b>	<b>Others</b>	<b>13</b>
6.1	Subgrid-scale orography . . . . .	13
<b>7</b>	<b>Configuration</b>	<b>15</b>
7.1	run.def . . . . .	15
7.2	config.def . . . . .	16
7.3	gcm.def . . . . .	18
7.4	physiq.def . . . . .	19
7.5	traceur.def . . . . .	20
7.6	orchidee.def . . . . .	21

error Value needed explanation needed doubt

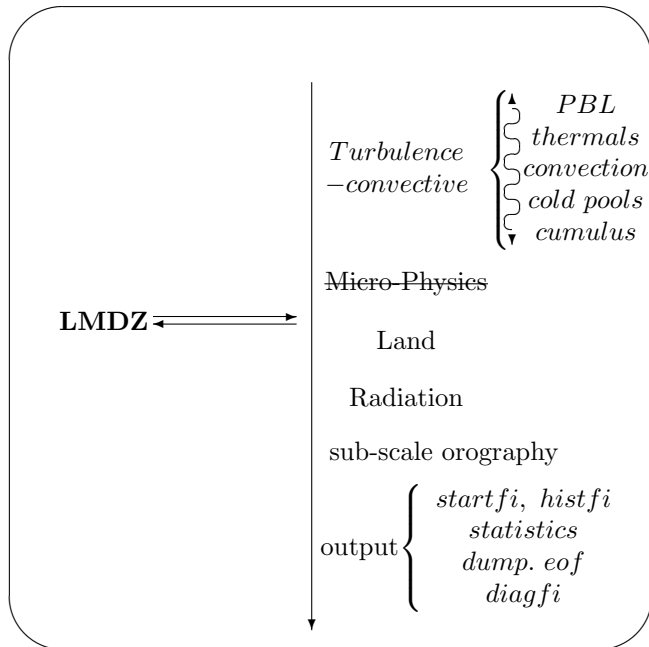


Figure 1: Schematic representation of the physics schemes used by LMDZ

## 1 Introduction

This document attempts to be a short introduction to the series of schemes that constitute the physical core of the *Laboratoire de Météorologie Dynamique Zoomed* (LMDZ, <http://lmdz.lmd.jussieu.fr/>) model, developed by the *Laboratoire de Météorologie Dynamique* (LMD, <http://www.ipsl.fr/en/Organisation/IPSL-Labs/LMD>), of the *Institute Pierre Simone Laplace* (IPSL, <http://www.ipsl.fr/en>) of the *Centre national de la recherche scientifique* (CNRS, <http://www.cnrs.fr/>).

The schemes are basically developed initially by 1D case study simulations and re-tuned for the 3D runs.

Text of this document is partially taken directly (as it is) from the cited articles. Due to the large amount of this kind of text, no distinction with respect author's original one is done. This document describes the physical configuration of LMDZ known as LMDZ-B [HGR<sup>+</sup>13]

## 2 Radiation scheme

Radative scheme in LMDZ is an adapted version from [Mor91]. At the time of this document is being written, LMD team is working to implement the rrtm scheme (version? rrtm, rrtmg?)

Are there in LMDZ independent vertical layers used for the radiation scheme, or does it use the same ones of the model vertical discretization?

How does LMDZ incorporate the time-evolution of GHG gases? How does it deal with different scenarios?

Is the outputted cloud fraction the same one 'used' by the radiative scheme?

Radiation scheme has suffered different evolutions from a first one (of 1979, EC1) with the interaction between line absorption and scattering using a photon path distribution method to the last version (1989, C3, the implemented one) summarized in table 1

The transmission functions  $\tau$  are computed with the help of an empirical function [Gel77] for the reduced ( $u_r$ ) and unreduced ( $u$ ) amounts of absorbers ( $CO_2$ ,  $CH_4$ ,  $N_2O$ ,  $CO$  and  $CO_2$ ):

$$-\ln \tau = \frac{au}{\sqrt{1 + bu^2/u_r}} + cu_r \quad (1)$$

where  $cu_r$ , continuum absorption, coefficients  $a$ ,  $b$  and  $c$  incorporate the temperature dependence of the absorption (linearly dependent on  $1/T$ ) fitted to the experimental data from [MFS<sup>+</sup>72, Vig53].

Last version of the scheme has evolved from narrow-band models to high spectral resolution (225 spectral intervals in the longwave, 208 in the shortwave) ones. Which have been compared to line-by-line calculations [SC81] and in situ measurements. These detailed models were then degraded by introducing simplifying assumptions, making them more computationally efficient. In that process, the sensitivity of the outputs (fluxes and heating/cooling rates) to the various assumptions have been monitored [MF85, MF86]. In the longwave, those studies showed that one of the causes for major systematic errors is the use of wide spectral intervals which tend to overestimate the effects of the strong lines, thus giving a poor representation of the temperature and pressure dependence of the absorption.

Clear-sky longwave fluxes are evaluated with an emissivity method incorporating a parameterization giving a correct representation of the temperature and pressure dependence of the absorption [MSF86]. Clouds are introduced as gray bodies with a longwave emissivity depending on the cloud liquid water path, following [Ste78].

Shortwave fluxes are computed using a photon path distribution method to separate the contributions of scattering and absorption processes to the radiative transfer. Scattering is treated with a delta-Eddington approximation. Transmission functions are developed as Padé approximates. Coefficients for the molecular absorption are calculated from the 1982 version of the Air Force Geophysics Laboratory (AFGL) line parameters compilation. Cloud shortwave radiative parameters are the optical thickness and single-scattering albedo linked to the cloud liquid water path, and a prescribed asymmetry factor [Fou88]. In EC3 a distinction is made between various cloud types by defining the optical thickness as a function not only of the liquid water path in the cloud, but also of the effective radius  $r_e$  of the cloud particles, with  $r_e$  varying with height from 5  $\mu m$  in the planetary boundary layer to 40  $\mu m$  at 100  $hPa$ . This last feature is an empirical attempt at dealing with the variation of cloud type with height, as smaller water droplets are observed in low-level stratiform clouds, whereas larger particles are found in cumuliform and cirriform clouds. This radiation scheme has already been extensively tested in the ECMWF model [Mor90] and was introduced in the operational forecast model on May 2, 1989.

### 3 PBL, convection and cumulus schemes

In LMDZ a big effort in the turbulent and convection physics of the model has been done. Previous version of the model [known as LMDZ-A HFC<sup>+</sup>13] used the Mellor-Yamada pbl scheme [MY74] in combination with Emanuel's convective one [Ema93]. In a new set of physics schemes [LMDZ-B HGR<sup>+</sup>13] huge modifications have been introduced and in this version (LMDZ v5): on the PBL scheme '*Thermals*' are tacking into account [HCM02], a new scheme representing cold pools due to precipitating water evaporation (wakes) have been included [GL09] which at the same time a new closure methodology has been introduced in Emanuel's convection [based on sub-clouds processes GPT04]. All these schemes interact among each other. By this reason, in LMDZ-B there is not such split of three specific schemes (pbl, deep convection and cumulus) such in other models.

All these changes have been reported with a huge positive impact. For example, a better representation of the low level clouds is attained, the daily cycle of precipitation over continents presents a maximum closer to the afternoon fixing a well known bias of the models [see HGR<sup>+</sup>13].

Semi-detailed explanation of the schemes will be done following the same scheme as in [HFC<sup>+</sup>13].

The new set of parameterizations relies on the separation of three distinct scales for the turbulent and convective subgrid-scale vertical motions:

1. The small scale (10100 m), associated with random turbulence, dominant in particular in the surface layer.
2. The boundary layer height (500 m-3 km) that corresponds to the vertical scale of organized structures of the convective boundary layer.
3. The deep convection depth (1020 km) of cumulonimbus, meso-scale convective systems or squall lines.

The first two scales dominate the vertical subgrid-scale transport in the boundary layer. In the '*B physics*', the parameterization of this vertical transport relies on the combination of a diffusion scheme for small scale turbulence and a mass-flux model of the organized structures of the convective boundary layer, the so-called '*thermal plume model*' [HCM02, RH08].

Table 1: Summary of ECMWF radiative scheme characteristics for clear/covered sky and short/longwave spectrum

Sky	wave	characteristic	method
Clear sky	shortwave <sup>a</sup>	Rayleigh scattering	Parametric expression of the Rayleigh optical thickness
		Aerosol scattering and absorption	Mie parameters for five types of aerosols based on climatological models [WMO84]
		Gas absorption	From AFGL 1982 compilation of line parameters
		$H_2O$	One interval
		Uniformly mixed gases <sup>b</sup>	One interval
		$O_3$	Two intervals
	longwave <sup>c</sup>	$H_2O$	Six spectral intervals, <i>e</i> - and <i>p</i> -type continuum absorption included between 350 and 1250 $cm^{-1}$
		$CO_2$	Overlap between 500 and 1250 $cm^{-1}$ in three intervals by multiplication of transmission
		$O_3$	Overlap between 970 and 1110 $cm^{-1}$
		Aerosols	Absorption effects using an emissivity formulation
Cloudy sky	shortwave	Droplet absorption and scattering	Employs a delta-Eddington method with $\tau$ and $w$ determined from LWP, and preset $g$ and $r_e$
		Gas absorption	Included separately throughout the photon path distribution method
	longwave	scattering	Neglected
		Droplet absorption	from LWP using an emissivity formulation
		Gas absorption	As for clear sky, longwave above

<sup>a</sup>two-stream formulation is employed together with photon path distribution method [FB80] in two spectral intervals (0.25-0.68 & 0.68-4.0  $\mu m$ )

<sup>b</sup> $CO_2$ ,  $CH_4$ ,  $N_2O$ ,  $CO$  and  $O_2$

<sup>c</sup>Broad-band flux emissivity method with six intervals covering the spectrum between zero and 2620  $cm^{-1}$ . Temperature and pressure dependence of absorption following [MSF86]. Absorption coefficients fitted from AFGL 1982.

### 3.1 Planetary Boundary Layer scheme

Main characteristics combination of a:

- eddy diffusion
- *'thermal plume model'*: mass-flux representation of the organized thermal structures of the convective boundary layer

The boundary layer parameterization now relies on the combination of a classical eddy diffusion [Yam83] with a mass-flux representation of the organized thermal structures of the convective boundary layer, the so-called [*'thermal plume model'* HCM02, RH08]. It enables one to represent the upward convective transport in the mixed layer although this layer is generally marginally stable [HCM02], solving a long recognized limitation of eddy diffusion [Dea66]. Mass-flux schemes account reasonably well for the organized structures (thermal plumes, or rolls) of the convective boundary layer. Their properties are used in the new model version for coupling with deep convection and also to better parameterize the boundary layer clouds [RH08, JHRC11].

The computation of the eddy diffusivity  $\mathcal{K}_z$  is based on a prognostic equation for the turbulent kinetic energy, according to [Yam83]. It is mainly active in practice in the surface boundary layer, typically in the first few hundred meters above surface.

The mass flux scheme represents an ensemble of coherent ascending thermal plumes in the grid cell as a mean plume. A model column is separated in two parts: the thermal plume and its environment. The vertical mass flux in the plume  $f_{th} = \rho \alpha_{th} w_{th}$  (where  $\rho$  is the air density,  $w_{th}$  the vertical velocity in the plume and  $\alpha_{th}$  its fractional coverage) varies vertically as a function of lateral entrainment  $e_{th}$  (from environment to the plume) and detrainment  $d_{th}$  (from the plume to the environment):

$$\frac{\partial f_{th}}{\partial z} = e_{th} - d_{th} \quad (2)$$

For a scalar quantity  $q$  (total water, potential temperature, chemical species, aerosols), the vertical transport by the thermal plume (assuming stationarity) reads:

$$\frac{\partial f_{th} q_{th}}{\partial z} = e_{th} q - d_{th} q_{th} \quad (3)$$

$q_{th}$  being the concentration of  $q$  inside the plume (air is assumed to enter the plume with the concentration of the large scale, which is equivalent to neglect the plume fraction  $\alpha_{th}$  in this part of the computation). The time evolution of  $q$  finally reads:

$$\frac{\partial q}{\partial t} = -\frac{1}{\rho} \frac{\partial \overline{\rho w' q'}}{\partial z} \quad (4)$$

with

$$\overline{\rho w' q'} = f_{th} (q_{th} - q) - \rho \mathcal{K}_z \frac{\partial q}{\partial z} \quad (5)$$

The vertical velocity  $w_{th}$  in the plume is driven by the plume buoyancy  $g(\theta_{th} - \theta)/\theta$ . The thermal plume fraction is also an internal variable of the model. The computation of  $w_{th}$ ,  $\alpha_{th}$ ,  $e_{th}$  and  $d_{th}$  is a critical part of the code. Detailed tests on two different versions of the  $e_{th}$  and  $d_{th}$  computation are presented in detail by [RH08] and [RHCJ10] respectively.

#### 3.1.1 Thermal

Let us consider a vertical profile of potential temperature typical of the Convective Boundary Layer (CBL), with an unstable surface layer (SL) of height  $z_s$ , a neutral mixed layer (ML) topped by a stable atmosphere (entrainment zone plus free atmosphere) as shown in Fig. 2. Although the entrainment layer may or may not be an inversion layer, we will use the classical notation  $z_i$  for the height of the top of the mixed layer [following chapter 1 Stu88].

In this idealized environment, the thermal is introduced as a simple plume of buoyant air coming from the SL. Buoyancy is expressed as the gravity times the relative difference between virtual potential temperature inside and around the thermal plume. The virtual potential temperature is

$$\theta_v = T \left( \frac{p_0}{p} \right)^\kappa (1 + 0.61q) \quad (6)$$

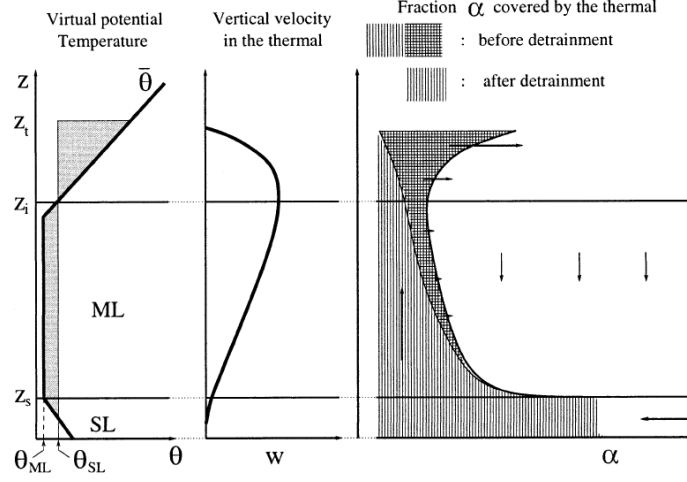


Figure 2: Schematic representation of a thermal from [HCM02]

where  $T$  is the air temperature,  $p_0 = 10^5 \text{ Pa}$ ,  $\kappa = 0.287$ , and  $q$  is the specific humidity in  $\text{kgkg}^{-1}$ . In this section, in order to avoid the use of multiple indices, the virtual potential temperature is notified  $\theta$ .

If the plume does not mix with its environment, its virtual potential temperature is that of the SL,  $\theta_{SL}$ . If, in addition, the thermal is assumed to be stationary and frictionless, the vertical velocity inside the plume, in absence of phase change of water, is given by

$$\frac{dw}{dt} = w \frac{\partial w}{\partial z} = g \frac{\theta_{SL} - \theta_{ML}}{\theta_{ML}} \quad (7)$$

(horizontal pressure differences between the plume and its environment are neglected). The air is uniformly accelerated in the ML until the level where the mean potential temperature  $\bar{\theta}(z)$  exceeds  $\theta_{SL}$ . This level will be retained for definition of  $z_i$ . At this level, the square of the vertical velocity  $w_{max}$  obtained by vertically integrating Eq. 7 over the depth of the CBL is twice the convective available potential energy (CAPE) defined as

$$CAPE = \int_0^{z_i} dz g \frac{\theta_{SL} - \theta_{ML}}{\theta_{ML}} \quad (8)$$

Above  $z_i$ ,  $w$  is still positive (overshooting) but decreases to finally vanish at the height  $z_t$  (top), where

$$\int_0^{z_t} dz g \frac{\theta_{SL} - \bar{\theta}}{\bar{\theta}} = 0. \quad (9)$$

The integral corresponds to the shaded area on the left-hand side of Fig. 2 and the CAPE to that part of the integral below  $z_i$ . After reaching  $z_t$ , air parcels coming from the plume are heavier than the environment and should sink again. This will not be considered here.

What is required for transport computations is not the vertical velocity but rather the mass flux per unit area,  $f = \alpha \rho w$ , where  $\alpha$  is the fraction of the horizontal surface covered by ascending plumes and  $\rho$  is the air density. As a first step, we assume that  $f$  is constant within the ML (no detrainment). In order to determine this constant value, it is necessary to invoke the geometry of the thermal cell. Results will depend on geometry of the plume [for further details see HCM02].

### 3.1.2 Cold pools

The wake model is fully described in [GL09, GLC09]. Only a short descriptive view of the scheme is presented here.

The model represents a population of identical circular cold pools (the wakes) with vertical frontiers over an infinite plane containing the grid cell. The wakes are cooled by the convective precipitating downdrafts, while the air outside the wakes feeds the convective saturated drafts (see figure 3).

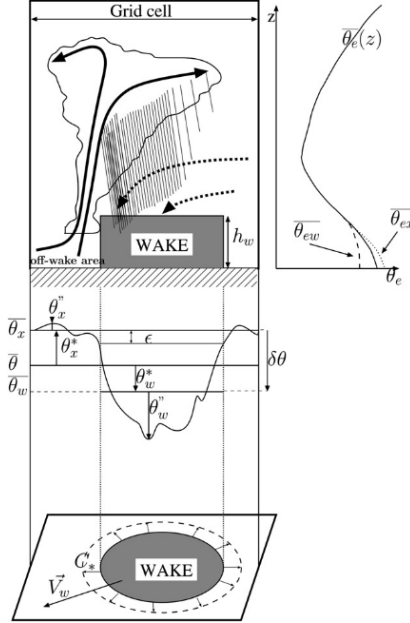


Figure 3: Schematic representation of a wake from [GL09]

The wake centers are assumed statistically distributed with a uniform spatial density  $\mathcal{D}_{wk}$ . The wake state variables are their fractional coverage  $\sigma_w$  ( $\sigma_w = \mathcal{D}_{wk}\pi r^2$ , where  $r$  is the wake radius), the potential temperature difference  $\delta\theta(p)$  and the specific humidity difference  $\delta q_v(p)$  between the wake region ( $w$ ) and the off-wake region ( $x$ ).  $\delta\theta(p)$  and  $\delta q_v(p)$  are non zero up to the homogeneity level  $p_h = 0.6p_s$  (where  $p_s$  is the surface pressure). Above  $p_h$  the sole difference between ( $w$ ) and ( $x$ ) regions lies in the convective drafts (saturated drafts in ( $x$ ) and unsaturated ones in ( $w$ )).

Wake air being denser than off-wake air, wakes spread as density currents, inducing a vertical velocity difference  $\delta w(p)$  between regions ( $w$ ) and ( $x$ ) ( $\delta w(p) > 0$ ). The vertical profile  $\delta w(p)$  is imposed piecewise linear. Especially, between surface and wake top (the altitude  $h_w$  where  $\delta\theta$  crosses zero) the slope corresponds to wake spreading without lateral entrainment nor detrainment.

The wake geometrical changes with time are due to the spread, split, decay and coalescence of the wakes. Split, decay and coalescence are merely represented by imposing a constant density  $\mathcal{D}_{wk}$  and by assuming that when  $\sigma_w$  reaches a maximum allowed value ( $= 0.5$ ) some wakes vanish (i.e. mix with the environment) while others split so that the fractional cover  $\sigma_w$  stays constant. The spreading rate of the wake fractional area  $\sigma_w$  reads:

$$\partial_t \sigma_w = 2C_* \sqrt{\pi \mathcal{D}_{wk} \sigma_w} \quad (10)$$

where  $C_*$ , the mean spread speed of the wake leading edges, is proportional to the square root of the *Wake Potential Energy WAPE*:  $C_* = \kappa_* \sqrt{2WAP E}$  and  $WAP E = -g \int_0^{h_w} \frac{\delta\theta_x}{\theta_v} dz$ , where,  $\kappa_*$ , the spread efficiency, is a tunable parameter in the range  $1/3 - 2/3$  and  $\theta_v$  is the virtual potential temperature.

The energy and water vapor equations are expressed at each level yielding prognostic equations for  $\delta\theta(p)$  and  $\delta q_v(p)$  as well as contributions to the average temperature  $\bar{\theta}$  and average humidity  $\bar{q}_v$  equations.

The convective scheme is supposed to provide separately the apparent heat sources due to saturated drafts and to unsaturated drafts, which makes it possible to compute the differential heating and moistening feeding the wakes.

There are not interactions among weaks?

## 3.2 Deep convection

Main characteristics as combination of:

- Emanuel's scheme
- New closure: sub-cloud processes: ALE, CIN, ALP from 'thermal plume model' and cold pool parameterizations

[Ema91] convection scheme is the base for the deep convection in LMDZ, but with a modification in its closure methodology based on the sub-cloud processes. The coupling of the convective parameterization with those of sub-cloud processes is done through the notions of *Available Lifting Energy* (ALE, which must overcome the *Convective INhibition*, or CIN, for triggering) and *Available Lifting Power* (ALP) that controls the convective closure. Both quantities are computed from internal variables of the 'thermal plume model' and of a new parameterization of the cold pools created by re-evaporation of convective rainfall in the sub-cloud layer [GL09, GLC09].

This version uses the buoyancy sorting mass-flux scheme of [Ema93], with modified mixing [GPT04] and splitting of the tendencies due to saturated and unsaturated drafts. The precipitation efficiency is computed as a function of the in-cloud condensed water and temperature following [EuR99]. It is bounded by a maximum value  $ep_{max}$  which is slightly less than unity to allow some cloud water to remain in suspension in the atmosphere instead of being entirely rained out [BE01].

The ALE allows to overcome the *Convective INhibition* (CIN) so that convection is triggered when  $ALE > |CIN|$ . The closure consists in prescribing the mass flux  $M$  at the top of the inhibition zone as:

$$M = \frac{ALP}{2w_B^2 + |CIN|} \quad (11)$$

where  $w_B$  is the updraft speed at the level of free convection. The original constant value  $w_B = 1m/s$  was replaced by a function of the level of free convection as explained below.

In this version, two processes are taken into account for both ALE and ALP: (1) the ascending motions of the convective boundary layer, as predicted by the thermal plume model and (2) the air lifted downstream of gust fronts. ALE is the largest of the lifting energies provided by the two processes:  $ALE = \max(ALE_{th}, ALE_{wk})$  where  $ALE_{th}$  scales with  $w_{th}^2$  and  $ALE_{wk} = WAPE$  (see eq. 10). ALP is the sum of the lifting powers provided by the two processes:  $ALP = ALP_{th} + ALP_{wk}$  where  $ALP_{th}$  scales with  $w_{th}^3$  and  $ALP_{wk}$  scales with  $C_*^3$  (see eq. 10).

This coupling between cold pools (generated by convection) and convection (triggered in turn and fed by cold pools) allows for the first time to get an autonomous life cycle of convection, not directly driven by the large scale conditions.

### 3.3 Cumulus scheme

It is based on a bi-gaussian statistical cloud scheme (Jam et al., 2011) **This article does not exist!!**

The fractional cloudiness  $\alpha_c$  and condensed water  $q_c$  are predicted by introducing a subrid-scale distribution  $P(q)$  of total water  $q$  so that:

$$\alpha_c = \int_{q_{sat}}^{\infty} dq P(q) \quad (12)$$

$$q_c = \int_{q_{sat}}^{\infty} (dq q - q_{sat})P(q) \quad (13)$$

where  $q_{sat}(T)$  is the grid averaged saturation specific humidity in the mesh.

For deep convection (see scheme in figure 4), we assume that the subgrid-scale condensation and rainfall can be handled by the Emanuel scheme, so that this statistical cloud scheme is used only to predict the fractional cloudiness for the radiative transfer. Following [BE01], the in-cloud water ( $q_{inc} = q_c/\alpha_c$ ) predicted by the convective scheme is used, through an inverse procedure, to determine the variance  $\sigma$  of a generalized log-normal function bounded at 0. With this particular function, the skewness of  $P(q)$  increases with increasing values of the unique width parameter  $\xi = \sigma/q$ .

For other types of clouds, the statistical cloud scheme is used to compute not only the cloud properties for radiation but also 'large scale' condensation.

If the thermal plume is not active in the grid box (in practice if  $f_{th} = 0$  see equation 2), the width parameter  $\xi$  of the generalized log-normal function is specified as a function of pressure:  $\xi(p)$  increases linearly from 0 at surface to  $\xi_{600} = 0.002$  at 600 hPa, then to  $\xi_{300} = 0.25$  at 300 Pa. It is kept constant above.

When  $f_{th} > 0$  in the grid box, two options are available. Either we use the [BE01] procedure to invert the width parameter  $\xi$  from the knowledge of the condensed water computed in the thermal plumes (like what is done for deep convection) or we use a new statistical cloud scheme proposed by [JHRC11] in which the sub-grid scale distribution of the water saturation deficit (rather than total water) is parameterized as the sum of two Gaussian functions,



representing the variability within and outside the thermal plume respectively. The width of each Gaussian varies as a function of the thermal plume fractional cover  $\alpha_{th}$  and of the contrast in saturation deficit between the plume and its environment.

A fraction  $f_{iw}$  of the condensed water  $q_c$  is assumed to be frozen. This fraction varies as a function of temperature from  $f_{iw} = 0$  at  $273.15\text{ K}$  to  $f_{iw} = 1$  at  $258.15\text{ K}$ . The condensed water is partially precipitated. Derived from [ZK97] formula for an anvil model, the associated sink is

$$\frac{dq_{iw}}{dt} = \frac{1}{\rho} \frac{\partial}{\partial z} (\rho w_{iw} q_{iw}) \quad (14)$$

where  $w_{iw} = \gamma_{iw} \times w_0$ ,  $w_0 = 3.29(\rho q_{iw})^{0.16}$  being a characteristic free fall velocity (in  $m/s$ ) of ice crystals given by [HD90] and  $\gamma_{iw}$  a parameter introduced for the purposes of model tuning ( $\rho$  in  $kg/m^3$ ).

For liquid water, following [Sun78], rainfall starts to precipitate above a critical value  $clw$  ( $0.6\text{ g/kg}$  in the reference version) for condensed water, with a time constant for auto-conversion  $\tau_{convers}$  ( $= 1,800\text{ s}$ ) so that

$$\frac{dq_{lw}}{dt} = -\frac{q_{lw}}{\tau_{convers}} \left[ 1 - e^{-(q_{lw}/clw)^2} \right] \quad (15)$$

A fraction of the precipitation is re-evaporated in the layer below and added to the total water of this layer before the statistical cloud scheme is applied. For ice particles, we assume that all the precipitation re-evaporates. For liquid water, following [Sun88], we assume that

$$\frac{\partial P}{\partial z} = \beta [1 - q/q_{sat}] \sqrt{P} \quad (16)$$

where  $P$  is the precipitation flux, and  $\beta$  a tunable parameter.

The effective radius of cloud droplets depends on the aerosol concentration which is specified as a function of space and season as explained by [DFD<sup>+</sup>13] this issue. The effective radius of ice crystals varies linearly as a function of temperature between  $er_{iw,max}$  at  $0\text{ }^\circ\text{C}$  and  $er_{iw,min}$  at  $-84.1\text{ }^\circ\text{C}$ .

The second point concerns the treatment of stratocumulus. Although some encouraging work is done currently on the thermal plume model in that direction, the current version does not represent properly strato-cumulus clouds. Strato-cumulus are known to be especially prominent at the eastern side of tropical oceans. On the other hand, the [Yam83] scheme alone performs quite well for those particular conditions. A kludge is thus introduced in the model, which consists in identifying the atmospheric columns with a sharp temperature inversion at the boundary layer top, and turning off the thermal plume model in those particular cases. In practice, if

$$\frac{T\partial\theta}{\theta\partial p} < -0.08\text{K/Pa} \quad (17)$$

then the thermal plume parametrization is arbitrarily switched off. This test is in fact inherited from the standard LMDZ5 model where it was used to switch between two different computations of the Kz coefficient with the same goal of contrasting the regions of strato-cumulus and trade wind cumulus on tropical oceans.

## 4 Micro-Physics scheme

No microphysics scheme is set up in LMDZ.

Meaning that no water species (drops,  $\overset{\longleftarrow}{\text{ice}} \leftrightarrow \text{liquid} \leftrightarrow \text{vapor}$ , graupel, snow, supercooled water,...) dynamics can occur in the LMDZ model

Look in WRF which is the simplest option

What about diabatic processes inside the plume and wake schemes?

## 5 Land scheme

What if Orchidee is not set up? SVAT SECHIBA?

$$\text{Cumulus} \left\{ \begin{array}{l}
\text{Deep convection} : \text{Emanuel} + \text{sub-cloud closure} \\
\text{other} : \text{statistical, } \xi \left\{ \begin{array}{l}
\left\{ \begin{array}{l} \text{Emanuel} \\ (PDF_{inside} + PDF_{outside}) |_{H_2O \text{ sat. deficit}} \end{array} \right. \text{plume active} \\
\left\{ \begin{array}{l} \text{lin. up to 0.002} \\ \text{lin. up to 0.25} \\ \text{ct. 0.25} \end{array} \right. \begin{array}{l} p \geq 600 \text{ hPa} \\ 600 \text{ hPa} > p \geq 300 \text{ hPa} \\ p < 300 \text{ hPa} \end{array} \text{plume inactive} \end{array} \right. \\
\text{Strato-cumulus} : \text{huge } \frac{T\partial\theta}{\theta\partial p} \text{ Switch off plume}
\end{array} \right.$$

Figure 4: Schematic representation of the diagram flow for the cumulus parameterization

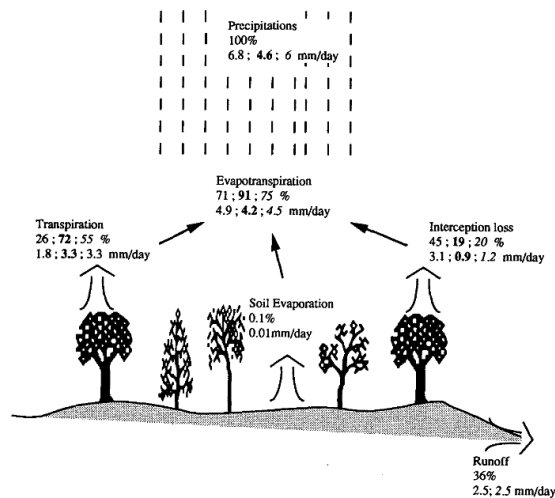


Figure 5: Example of water balance (Amazonian) for a given precipitation amount and the respective percentages from measured values [first, bold Shu88] and simulated [second, italic SSR<sup>+</sup>89] from [DLP93]

## 5.1 SVAT SECHIBA

Surface-vegetation-atmosphere transfer (SVAT) SECHIBA [DLP93, dRP98] has been developed as a set of surface parameterizations for the LMDZ. SVAT simulate exchanges of sensible, latent and kinetic energy at the surface. SECHIBA describes exchanges of energy and water between the atmosphere and the biosphere, and the soil water budget. In its standard version, SECHIBA contains no parameterization of photosynthesis. Time step of the hydrological module is of the order of 30 min.

For each grid point eight land surface types (bare soil plus seven vegetation classes) are defined, each of them covering a fractional area of the grid box and allowed to be found simultaneously. Over each of these covers the transfers are computed: evaporation from soil, transpiration from plants through a resistance defined by concepts of stomatal resistance and architectural resistance, and interception loss from the water reservoir over the canopy (see an schematic representation in figure 5). These fluxes are then averaged over the period box to derive the total amount of water vapor that is transferred to the first level of the atmospheric model. Parameterization of soil water allows for the moistening of an upper layer, of variable depth, during a rainfall event. The scheme requires prescription of a restricted number of parameters: seven for each class of vegetation **not found** and four for the soil **not found**.

SECHIBA represents:

- *latent heat flux*: exchanges of water vapor between the soil/vegetation system and the atmosphere
- *soil hydrological cycle*

Table 2: Equations for each element of the latent heat flux decomposition from [DLP93]

	$\Delta q$	$\alpha$	$\sum_{\ell} r_{\ell}$
<b>Snow sublimation</b>	$q_{sat}(T_g) - q_a$	$\frac{S_n}{S_{cr}}$	$r_a$
<b>Soil evaporation</b>	$h_g q_{sat}(T_g) - q_a$	$\left(1 - \frac{S_n}{S_{cr}}\right) (1 - \sigma_f)$	$r_a + r_g$
<b>Canopy transpiration</b>	$h_g q_{sat}(T_g) - q_a$	$\left(1 - \frac{S_n}{S_{cr}}\right) \sigma_f \left(1 - \left(\frac{W_{dew}}{W_{dmax}}\right)^{2/3}\right)$	$r_a + r_0 + r_c$
<b>Evaporation of foliage water</b>	$q_{sat}(T_g) - q_a$	$\left(1 - \frac{S_n}{S_{cr}}\right) \sigma_f \left(\frac{W_{dew}}{W_{dmax}}\right)^{2/3}$	$r_a + r_0$

Table 3: Canopy parameters prescribed in SECHIBA

Parameters	Tundra	Grassland	Grassland + shrub cover	Grassland + tree cover	Decidius forest	Evergreen forest	Rain forest
LAI Summer	1	2	2.5	3.5	5	4	8
LAI Winter	0	1.5	1	1.5	0	3	8
$r_0$ ( $sm^{-1}$ )	10	2	2.5	3	40	50	25
$k_0$ ( $kgm^{-2}s^{-1} 10^{-5}$ )	5.0	30.0	25.0	28.0	25.0	12.0	24.0

Vegetation is treated as a single element in the equations. However, because different fractions of vegetation types can coexist in the grid box, certain vegetation contributions such as evapotranspiration will be the result of the combination of all the classes of vegetation within the grid box.

For sensible heat flux calculations vegetation and soil are considered as a single element.

Total latent heat flux ( $E_a$ ) would be the weighted combination of snow sublimation ( $E_s$ ), soil evaporation ( $E_g$ ), canopy transpiration ( $E_{tr}$ ) and evaporation of foliage water ( $E_i$ , intercepted precipitation and dew). Each of one is computed following:

$$E_{s,g,tr,i} = \alpha_{s,g,tr,i} \rho \frac{\Delta q_{s,g,tr,i}}{\sum_{\ell} r_{\ell}} \quad (18)$$

where  $\Delta q_{s,g,tr,i}$  is the gradient of specific humidity between the evaporating surface and the overlying air, and limited by a sum of resistances ( $r_{\ell}$ ).  $\alpha_{s,g,tr,i}$  is the fraction of grid box evaporating and  $\rho$  air density. This formulation was introduced by [Mon63] and is known by the 'big-leaf' or 'single-leaf' model.

There is an *aerodynamic resistance* ( $r_a$ ) that opposes the transfer of water vapor which is inversely proportional to the product of the surface drag coefficient ( $C_d$ ) and the wind speed ( $V_a$ ).

$$r_a = \frac{1}{C_d V_a} \quad (19)$$

*Soil evaporation* is calculated following a *bulk aerodynamic method* (see section 5.1.1) as a combination of the surface relative humidity ( $h_g$ ) and a soil resistance ( $r_g$ , see equation 20) which are function of the soil moisture. Soil resistance has a dependency on the soil type tacking its values from observations [Mat83b, Mat83a, Mat84].

$$r_g = r_{soil} \frac{D_u W_{umax} - W_u}{D_t W_{umax}} \quad (20)$$

The *architectural resistance* ( $r_0$ ) would take into account the aerodynamic resistance between leaves and canopy top. In this scheme canopy is defined as a single layer, and a resistance is included following [SK91]. Values are taken from a Perrier (personal communication) and are function of the vegetation type (see table 3)

The *canopy resistance* ( $r_c$ , see equation 21) summarizes the bulk stomatal and leaf aerodynamical resistances. It depends on the solar radiation ( $R_s$ ) and the water vapor concentration deficit ( $\delta c$ ) simulated above canopy being

inversely proportional to the single-sided Leaf Area Index (LAI). Is empirically based [LLL80, Jar76], and in this scheme it does not depend on soil moisture.

$$r_c = \frac{1}{LAI} \frac{R_s + R_{s0}}{R_s} \frac{a + \lambda \delta c}{k_0} \quad (21)$$

For the gradients of specific humidity between evaporating surface and the air above requires the computation of the *surface relative humidity* (srh). In the scheme srh is given as function of the soil water content and a retention coefficient ( $h_g$ ).

$$h_g = \exp\left(-c \frac{D_u}{D_t} \frac{W_{umax} - W_u}{W_{umax}}\right) \quad (22)$$

Part of the precipitated water can be intercepted by the foliage. A result of this, when leaves get wet, they can not transpire. This effect is taken into account and it depends on the incident rainfall and a maximum water storage ( $W_{dmax} = 0.5LAI$ ) which depends on the LAI index

$$\frac{\partial W_{dew}}{\partial t} = \sigma_f P_r - E_i \quad (23)$$

$$W_{dew} \leq W_{dmax}$$

The total soil depth is limited to the root zone. The maximum water that a soil grid point can hold is computed as the difference between the profiles of soil moisture at saturation and at wilting point. The soil has an upper dynamic layer with variable depth where all the dynamics occur ('*bulk method*', see section 5.1.1), acting the rest as a *reservoir*. When it rains soil is filled from top to bottom. Soil is dried when evapotranspiration is larger than precipitation. Runoff occurs when soil is saturated. Canopy transpiration ceases when soil is completely dry (i.e. at the wilting point). In SECHIBA only two soil layers are considered.

The *stomatal aperture* which determines the transpiration is given as a function of  $r_c$ ; LAI;  $R_{s0} = 125 \text{ Wm}^{-2}$ , half light saturation factor;  $a = 23 \times 10^{-3} \text{ kgm}^{-2}$ ;  $k_0$  and  $\delta c$  and  $\lambda = 1.5$ .  $a$ ,  $R_{s0}$  and  $\lambda$  are the same for all vegetation types due to the lack of measurements.

*Bare soils* are described by:

- $D_t = 1 \text{ m}$ , total depth (root zone)
- $W_{tmax} = 150 \text{ kgm}^{-2}$ , maximum amount of water it can hold (g.e.: 70-80 sand, 150 clay, 200 loam). A mean value was chosen.
- $r_{soil} = 33000 \text{ sm}^{-1}$ , resistance exerted by 1 m of dry soil. Averaged values from different kind of soils
- $c = 0.8$ , empirical constant used to compute srh from [Cho77]

### 5.1.1 Bulk aerodynamic method

Total evapotranspiration ( $E_a$ ) is proportional to the potential rate ( $E_p$ ). The coefficient of proportionality ( $\beta$ ) is a function of total soil moisture ( $W_t$ ) and it is known as '*aridity coefficient*':

$$E_a = \beta E_p, \quad \beta = \begin{cases} 1, & \text{if } W_t > W_c \\ \frac{W_t}{W_c}, & \text{if } W_t \leq W_c \end{cases} \quad (24)$$

where,  $W_c = 0.5W_{tmax}$ , critical amount of soil moisture, above which it is assumed that evapotranspiration takes place at the potential rate, and  $E_p$  is function of the gradient of specific humidity between the surface and the overlying air:

$$E_p = \rho \frac{q_{sat}(T_g) - q_a}{r_a} \quad (25)$$

where  $r_a$ , aerodynamic resistance (see equation 19). Water in the soil is held in only one reservoir, the root zone, which is filled from bottom to top by precipitation and emptied from top to bottom by evaporation. This is way it is called '*bucket*'. Runoff occurs only when the soil is saturated, that is, when  $W_t = W_{tmax}$

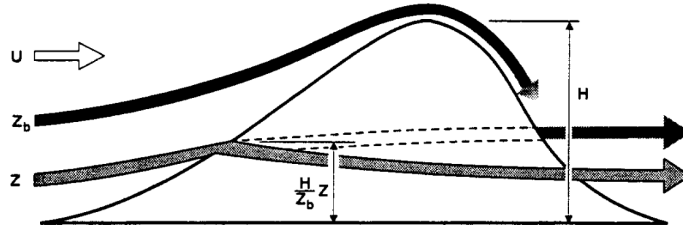


Figure 6: Schematic representation of the drag introduced by a mountain from [LM97]

## 5.2 Orchidee

Orchidee (<http://orchidee.ipsl.jussieu.fr/>) [KVdND<sup>+</sup>05] is a dynamic global vegetation model designed as an extension of an existing surface-vegetation-atmosphere transfer scheme which is included in a coupled ocean-atmosphere general circulation model. The dynamic global vegetation model simulates the principal processes of the continental biosphere influencing the global carbon cycle (photosynthesis, autotrophic and heterotrophic respiration of plants and in soils, fire, etc.) as well as latent, sensible, and kinetic energy exchanges at the surface of soils and plants. As a dynamic vegetation model, it explicitly represents competitive processes such as light competition, sampling establishment, etc. It can thus be used in simulations for the study of feedbacks between transient climate and vegetation cover changes, but it can also be used with a prescribed vegetation distribution. The whole seasonal phenological cycle is prognostically calculated without any prescribed dates or use of satellite data. Orchidee is based in three components:

- SVAT ESCHIBA [DLP93, dRP98] for the basics interchanges between atmosphere and soil
- Dynamic Global Vegetation Model (DGVM LPJ) [SSP<sup>+</sup>03] for the vegetation dynamics
- Saclay Toulouse Orsay Model for the Analysis of Terrestrial Ecosystems (STOMATE) based in *plant functional types (PFT)* for photosynthesis, carbon allocation, litter decomposition, soil carbon dynamics, maintenance and growth respiration and phenology

## 6 Others

### 6.1 Subgrid-scale orography

Effects of subgrid-scale orography (SSO) are accounted for both through drag and lifting effects on the obstacles and through generation and propagation in the atmosphere of gravity waves [LM97].

The assumption is that the mesoscale flow dynamics can be described by two conceptual models, whose relevance depends on the non-dimensional height of the mountain, viz.

$$H_n = \frac{NH}{|U|} \quad (26)$$

where  $H$  is the maximum height of the obstacle,  $U$  is the wind speed and  $N$  is the Brunt-Väisälä frequency of the incident flow (see figure 6).

At small  $H_n$ , all the flow goes over the mountain and gravity waves are forced by the vertical motion of the fluid. Suppose that the mountain has an elliptical shape and a height variation determined by a parameter  $b$  in the along-ridge direction and by a parameter  $a$  in the cross-ridge direction, such that

$$\gamma = a/b \leq 1 \quad (27)$$

then the geometry of the mountain can be written in the form

$$h(x, y) = \frac{H}{1 + x^2/a^2 + y^2/b^2} \quad (28)$$

In the simple case when the incident flow is at right angles to the ridge the surface stress due to the gravity wave has the magnitude

$$\tau_w = \rho_0 b \mathcal{G} \mathcal{B}(\gamma) N U H^2 \quad (29)$$

provided that the Boussinesq and hydrostatic approximations apply. In Eq. 29  $\mathcal{G}$  is a function of the mountain sharpness [Phi84], and for the mountain given by Eq. 28,  $\mathcal{G} \approx 1.23$ . The term  $\mathcal{B}(\gamma)$  is a function of the mountain anisotropy,  $\gamma$ , and can vary from  $\mathcal{B}(0) = 1$  for a two-dimensional ridge to  $\mathcal{B}(1) = \pi/4$  for a circular mountain.

At large  $H_n$  the vertical motion of the fluid is limited and part of the low-level flow goes around the mountain. The depth,  $Z_b$ , of this blocked layer, when  $U$  and  $N$  are independent of height, can be expressed as

$$Z_b = H \max \left( 0, \frac{H_n - H_{nc}}{H_n} \right) \quad (30)$$

where  $H_{nc}$  is a critical non-dimensional mountain height of order unity. The depth  $Z_b$  can be viewed as the upstream elevation of the isentropic surface that is raised exactly to the mountain top (Fig. 6). In each layer below  $Z_b$  the flow streamlines divide around the obstacle, and it is supposed that flow separation occurs on the obstacle's flanks. Then, the drag,  $\mathcal{D}_b(z)$ , exerted by the obstacle on the flow at these levels can be written as

$$\mathcal{D}_b(z) = -\rho_0 C_d l(z) \frac{U|U|}{2} \quad (31)$$

Here  $l(z)$  represents the horizontal width of the obstacle as seen by the flow at an upstream height  $z$ , and  $C_d$ , according to the free streamline theory of jets in ideal fluids, is a constant having a value close to unity [Kir77, Gur65]. According to observations,  $C_d$  can be nearer 2 in value when suction effects occur in the rear of the obstacle [Bat67]. In the proposed parametrization scheme this drag is applied to the flow, level by level, and will be referred to as the drag of the 'blocked' flow,  $\mathcal{D}_d$ . Unlike the gravity-wave-drag scheme, the total stress exerted by the mountain on the 'blocked' flow does not need to be known *a priori*. For an elliptical mountain, the width of the obstacle, as seen by the flow at a given altitude  $z < Z_b$ , is given by

$$l(z) = 2b \sqrt{\frac{Z_b - z}{z}} \quad (32)$$

In Eq. 32, it is assumed that the level  $Z_b$  is raised up to the mountain top, with each layer below  $Z_b$  raised by a factor  $H/Z_b$  (Fig. 6). This will lead, effectively, to a reduction of the obstacle width, as seen by the flow when compared with the case in which the flow does not experience vertical motion as it approaches the mountain. Then applying Eq. 31 to the fluid layers below  $Z_b$ , the stress due to the blocked-flow drag is obtained by integrating from  $z = 0$  to  $z = Z_b$ , viz.

$$\tau_b \approx C_d \pi b \rho_0 Z_b \frac{U|U|}{2} \quad (33)$$

However, when the non-dimensional height is close to unity, the presence of a wake is generally associated with upstream blocking and with a downstream Foehn (e.g. Fig. 6). This means that the isentropic surfaces are raised on the windward side and become close to the ground on the leeward side. If we assume that the lowest isentropic surface passing *over* the mountain can be viewed as a lower rigid boundary for the flow passing over the mountain, then the distortion of this surface will be seen as a source of gravity waves, and since this distortion is of the same order of magnitude as the mountain height, it is reasonable to suppose that the wave stress will be given by Eq. 29, whatever the depth of the blocked flow,  $Z_b$ , although it is clearly an upper limit to use the total height,  $H$ . Then, the total stress is the sum of a wave stress,  $\tau_w$ , a blocked-flow stress whenever the non-dimensional mountain height  $H_n > H_{nc}$ , i.e.

$$\tau \approx \tau_w \left\{ 1 + \frac{\pi C_d}{2 \mathcal{G} \mathcal{B}(\gamma)} \max \left( 0, \frac{H_n - H_{nc}}{H_n^2} \right) \right\} \quad (34)$$

The addition of low-level drag below the depth of the blocked flow,  $Z_b$ , enhances the gravity-wave stress term in Eq. 34 substantially. Two pair of correct values when compared with two numerical experiments would be  $C_d = 2$ ,  $H_{nc} = 0.4$  and  $C_d = 1$ ,  $H_{nc} = 0.75$ . In the later case, the smaller value of  $C_d$  is probably related to the reduction of

Table 4: Scheme card of the LMDZ5 physics B

<b>scheme</b>	<b>LMDZ-B</b>
radiation	ECMWF rad
pbl	Mellor and Yamada + Thermal plume model
convection	Emanuel + modified mixing and modified closure (ALP, ALE, CIN) + cold pool (wake)
clouds	Bonny and Emanuel statistical + prediction from subgrid-scale distribution of cloudiness and condensed water + statistical water saturation deficit model
micro-physics	$\emptyset$
land	SECHIBA/ORCHIDEE
others	Subgrid-scale orography (SSO)

upstream blocking in three-dimensional simulations. A larger  $H_{nc}$  corresponds to a reduction of the nonlinear effects due to the three-dimensional dispersion of the mountain waves. In the scheme, these effects are partly taken into account by allowing the value of  $C_d$  to vary with the aspect ratio of the obstacle, as in the case of separated flows around immersed bodies [Lan61], while at the same time setting the critical number  $H_{nc}$  equal to 0.5 as a constant intermediate value. Note also that for large  $H_n$ , Eq. 34 overestimates the drag in the three-dimensional case, because the flow dynamics become more and more horizontal, and the incidence of gravity waves is diminished accordingly. In the scheme a reduction of this kind in the mountain-wave stress could have been introduced by replacing the mountain height given in Eq. 29 with a lower 'cut-off' mountain height,  $H(H_{nc}/H_n)$ . Nevertheless, this has not been done in the parametrization scheme partly because a large non-dimensional mountain height often corresponds to slow flows for which the drag given by Eq. 34 is then, in any case, very small.

## 7 Configuration

LMDZ is configured throughout the use of different ASCII files [ver].def\ located at the same folder where the simulation is run. They attain different aspects of the configuration of the model, from period and domain of simulation to which values should be given to different constants inside the physical schemes.

A brief detail of the values inside these files is given with an attempt to keep track the meaning of certain values according to the equations described from the schemes.

### 7.1 run.def

Configuration ASCII file for the general configuration

```
## Fichier de configuration general
##
INCLUDEDEF=physiq.def
INCLUDEDEF=gcm.def
INCLUDEDEF=orchidee.def
INCLUDEDEF=output.def
INCLUDEDEF=config.def
```

---

calendar

---

ip_ebil_phy	1	(D: ?) meaning?
ip_ebil_dyn	1	(D: ?) meaning?
calend	earth_360d	Type of calendar to use (D: earth_360d, earth_360: 12 months of 30 days, dearth_365d: no leap years, earth_366d: leap years) does orbital parameters automatically adapt?
dayref	1	day julian with leap years? (units?) of the initial state (D: ?, g.e. 350 if 20 December)

anneeref	1980	year of the initial state (D: ?, in [YYYY] format)
nday	5	number of days of integration (D: ?, fraction?)
raz_date	0	reduction to zero of the initial date (D: ?)
output		
iconser	20	output period (in number of time-steps) of the control variables which are? (D: ?)
iecri	1	writing period (in days) of the history file (D: ?)
ok_dynzon	n	flag of 'dynzon' output (D: ?, n: no, y: yes) meaning?
periodav	30.	storage period (in days) of the 'dynzon' file (D: ?)
adjust	n	activation of the computation of balancing of the load (D: ?, n: no, y: yes) meaning?
use_filtre_fft	n	activation of the FFT filter (D: ?, n: no, y: yes) poles? different options?
prt_level	0	level of checking/debugging printing (D: ?)

Table 5: Configuration parameters of the file 'run.def'. 'D' stands for 'default' value. Showed values are from the test simulation LMDZ5 - BENCH48x36x19

## 7.2 config.def

Configuration ASCII file for the configuration

output						
OK_journe	y	daily (D: ?, n: no, y: yes)				
OK_mensuel	y	monthly (D: ?, n: no, y: yes)				
ok_hf	y	high frequency? (D: ?, n: no, y: yes)				
OK_instan	n	instantaneous? (D: ?, n: no, y: yes)				
ok_LES	n	LES (D: ?, n: no, y: yes)				
ok_regdyn	y	computation of the dynamical regimes in the pre-defined regions (D: ?, n: no, y: yes)				
What about restarts?						
Are all the variables written in all files?						
# To transform in the following line when it will be compatible with 'libGCM' meaning?						
phys_out_filekeys	y	y	n	y	n	file keys
phys_out_filenames	histmth	histday	histhf	histins	histLES	file names
phys_out_filetimesteps	5day	1day	1hr	6hr	6hr	file time steps values?
phys_out_filelevels	10	5	0	4	4	number of levels of output meaning?
phys_out_filetypes	ave(X)	ave(X)	ave(X)	inst(X)	inst(X)	output types values?
coupling with other modules						
type_ocean	force	option for coupling with the ocean (D: force, force: options?) does it use slab model otherwise?, does it modify SST?				
version_ocean	nemo	version of the ocean (D: ?, nemo: use Nemo model options?)				
VEGET	n	coupling with orchidee (D: n, n: no, y: yes) what uses otherwise?				
type_run	CLIM	type of run (D:AMIP, AMIP: ??, ENSP: ??, clim: ??)				
soil_model	y	activation of the soil model (D: ?, n: no, y: yes) is it incompatible with VEGET?				
radiative transfer						
iflag_radia	1	activation of the radiation (MPL) (D: 1, 0: without, 1: active)				
nbapp_rad	12	number of calls per day of the radiation routines (D: ?)				
orbital & geological era						



R_ecc	0.016715	eccentricity (D: ?)
R_peri	102.7	equinox (units?) (D: ?)
R_incl	23.441	inclination (degrees) of the rotation of the Earth (D: ?)
solaire	1366.0896	solar constant ( $Wm^{-2}$ ) (D: ?)
pmagic	0.008	additive factor (units?) for the albedo (D: ?)
ratio of Green House Gases		

		$CO_2$	$CH_4$	$N_2O$	$CFC - 11$	$CFC - 12$	
	D:	348.	1650.	306.	280.	484.	
co2_ppm	0.36886500E+03						$CO_2$ (ppm)
#RCO2=co2_ppm * 1.0e-06 * 44.011/28.97=	5.286789092164308E-04						meaning?
CH4_ppb	0.17510225E+04						$CH_4$ (ppb)
#RCH4=1.65E-06* 16.043/28.97=	9.137366240938903E-07						meaning?
N2O_ppb	0.31585000E+03						$N_2O$ (ppb)
#RN2O=306.E-09* 44.013/28.97=	4.648939592682085E-07						meaning?
CFC11_ppt	5.18015181E+01						$CFC - 11$ (ppt)
#RCFC11=280.E-12* 137.3686/28.97=	1.327690990680013E-09						meaning?
CFC12_ppt	0.99862742E+03						$CFC - 12$ (ppt)
#RCFC12=484.E-12* 120.9140/28.97=	2.020102726958923E-09						meaning?

effect of aerosols		
ok_ade	n	flag of the direct effect of the aerosol (D: ?, n: no, y: yes)
ok_aie	n	flag of the indirect effect of the aerosol (D: ?, n: no, y: yes)
aer_type	actuel	type of variation of the aerosol (D: ?, actuel: ??, preinD: ??, scenario: ??, annuel: ??) external file?
flag_aerosol	=0	type of the couple aerosol (D: 1, =1: ??, =2: only bc, =3: only pom, =4: only seasalt, =5: only dust, =6: all aerosol)
bl95_b0	1.7	parameter in the CDNC-maer link ( $\log_{10}(CDCN) = bl95\_b0 + bl95\_b1 \log(mSO_4)$ ) [BL95] (D: ?)
bl95_b1	0.2	parameter in the CDNC-maer link [BL95] (D: ?)
read_climoz	0 which file?	ozone reading (D: ?) 0: do not read an ozone climatology 1: read a single ozone climatology that will be used day and night 2: read two ozone climatologies, the average day and night climatology and the daylight climatology

COSP (CFMIP Observational Simulator Package, <http://cfmip.metoffice.com/COSP.html>)

Is the COSP package included in the LMDZ code? If yes which version?

ok_cosp	n	activation of the COPS simulator (D: ?, n: no, y: yes)
freq_COSP	10800.	frequency (in seconds?) of calling of the COSP simulator (D: ?)
ok_mensuelCOSP	y	outputting of monthly COSP file 'histmth-COSP.nc' (D: ?, n: no, y: yes)
ok_journeCOSP	y	outputting of daily COSP file 'histdayCOSP.nc' (D: ?, n: no, y: yes)
ok_hfCOSP	n	outputting of high frequency COSP file 'histhf-COSP.nc' (D: ?, n: no, y: yes)

ISCCP simulator <http://cfmip.metoffice.com/ISCCP.html>  
 Is the ISCCP package included in the LMDZ code? version?

ok_isccp	n	activation of the ISCCP simulator (D: ?, n: no, y: yes)
top_height	=1	selection of computation of clouds for the simulator when it uses the IR and/or VIS data and the algorithm ISCCP-D1 (D: ?) =1: IR-VIS algorithm =2: same as 1, plus " $p_{top}(ibox) = p_{full}(ilev)$ " =3: IR algorithm Hypothesis of covering (HR) used by the ISCCP simulator (D: ?)
overlap	3	1 Maximum overlap 2 Random overlap 3 Max/Random overlap

Differences between COSP & ISCCP?

Are active 'species' in the schemes? Do they interact with thermals, cold pools,...?

Computational cost of introduction of COSP and ISCCP?

Table 6: Configuration parameters of the file 'config.def'. 'D' stands for 'default' value. Showed values are from the test simulation LMDZ5 - BENCH48x36x19

### 7.3 gcm.def

Configuration ASCII file for the gcm configuration

day_step	240	number of time-steps per day multiple of 'iperiod' (D: ?)
iperiod	5	period for the Matsuno's time-step (D: ?, in number of time-steps)
dissipation		
idissip	5	dissipation period (D: ?, in number of time-steps)
lstdis	y	activation of the dissipative operator (D: ?, n: no, y: yes)
nitergdiv	1	number of iterations of the dissipation operator 'gradiv' (D: ?) <a href="#">meaning?</a>
nitergrot	2	number of iterations of the dissipation operator 'nxgradrot' (D: ?) <a href="#">meaning?</a>
niterh	2	number of iterations of the dissipation operator 'divgrad' (D: ?) <a href="#">meaning?</a>
tetagdiv	18000.	dissipation time (in <a href="#">seconds?</a> ) of the smallest long.d waves for u,v in 'gradiv' (D: ?)
tetagrot	18000.	dissipation time (in <a href="#">seconds?</a> ) for the smallest waves for u,v in 'nxgradrot' (D: ?)
tetatemp	18000.	dissipation time (in <a href="#">seconds?</a> ) of the smallest long.d waves for h in 'divgrad' (D: ?)
dissip_period	0	frequency of activation of the dissipation (D: ?, multiple of 'iperiod', 0 if it is done automatically)
coefdis	0.	coefficient ( <a href="#">units?</a> ) for 'gamdissip' (D: ?) <a href="#">meaning?</a>
purmats	n	selection of the temporal integration scheme (D: ?, y: Matsuno, n: Matsuno-leapfrog) flag of physics selection (D: ?)
iflag_phys	1	0: without physics (e.g. Shallow Water) 1: with physics (e.g. phylmd physics) 2: with recall to Newtonian inside the dynamics
read_start	y	flag indicating the use of starting files 'start.nc' and 'startphy.nc' (D: ?, y: yes, n: without. Initialization of fields is done by dynamics using 'iniacademic')
iphysiq	5	period of the physics in dynamical time-steps (D: ?, in combination with iflag_phys=1) <a href="#">Is the same for all schemes?</a>
nsplit_phys	1	number of time-steps of the physics (D: ?) <a href="#">Schemes can be run multiple times within the same time-step?</a>

ok_strato	n	flag indicating strato (D: ?, n: no, y: yes)
iflag_top_bound	0	sponge layer of the pressure levels with less than 100 times the pressure of the last level (D: ?)
tau_top_bound	5.e-5	coefficient (units?) for the sponge layer (value at the last level) (D: ?)
zoom	There is no flag for zoom no/yes?	
clon	0.	longitude (in degrees) of the center of the zoom (D: ?)
clat	45.	latitude (in degrees) of the center of the zoom (D: ?)
grossismx	1.0	magnification factor of the zoom according to the longitude (D: ?)
grossismy	1.0	magnification factor of the zoom according to the latitude (D: ?)
fxhyphb	y	selection of the function 'f(y)' of the zoom (D: ?, .true.: hyperbolic, .false.: sinusoidal)
dzoomx	0.15	extension in longitude (as fraction of the total zone) of the zoom zone (D: ?)
dzoomy	0.15	extension in latitude (as fraction of the total zone) of the zoom zone (D: ?)
taux	3.	rigidity of the zoom in X (D: ?)
tauy	3.	rigidity of the zoom in Y (D: ?)
ysin	y	kind of latitude dependence of function 'f(y)' (D: ?, n: latitude, y:sin(latitude) )

Table 7: Configuration parameters of the file 'gcm.def'. 'D' stands for 'default' value. Showed values are from the test simulation LMDZ5 - BENCH48x36x19

## 7.4 physiq.def

Configuration ASCII file for the physical schemes

#####

## Si=.T. , lecture du fichier limit avec la bonne annee [meaning?](#)

---

orographic parametres and cdrags

[Equivalence with \[LM97\]?](#)

[Is it called al time-steps?](#)

ok_limitvrai	n	(D: ?, n: no, y: yes) <a href="#">meaning?</a>
f_cdrag_stable	1.	Cdrags (units?) (D: ?) <a href="#">meaning?</a>
f_cdrag_ter	1.	Cdrags (units?) (D: ?) <a href="#">meaning?</a>
f_cdrag_oce	0.8	Cdrags (units?) (D: ?) <a href="#">meaning?</a>
cdmmax	2.5E-3	Cdrags (units?) (D: ?) <a href="#">meaning?</a>
cdhmax	2.0E-3	Cdrags (units?) (D: ?) <a href="#">meaning?</a>
ok_orodr	y	Orodr for the orography (D: ?, n: no, y: yes) <a href="#">meaning?</a>
ok_orolf	y	Orold for the orography (D: ?, n: no, y: yes) <a href="#">meaning?</a>
f_rugoro	0.	Rugoro (units?) (D: ?) <a href="#">meaning?</a>

Is it called all time-steps?

---

radiation

iflag_rrtm	0	activation of new radiation scheme RRTM (D: 0, 0: no, 1: yes)
------------	---	---

---

clouds

cld_lc_lsc	4.16e-4	precipitation threshold (units?) for the stratiform clouds (D: 2.6e-4)
cld_lc_con	4.16e-4	precipitation threshold (units?) for the stratiform clouds (D: 2.6e-4)
cld_tau_lsc	1800.	temporal constant (in seconds?) to remove lsc water (D: 3600.)
cld_tau_con	1800.	temporal constant (in seconds?) to remove convective water (D: 3600.)
ffallv_lsc	0.5	corrective factor for the falling of the ice cristals (D: 1)
ffallv_con	0.5	corrective factor for the falling of the ice cristals (D: 1)
coef_eva	2e-5	evaporation coefficient for the rain (D: 2.e-5)
reevap_ice	y	(D: n, n: no, y: yes) <a href="#">meaning?</a>
iflag_cldcon	3	computation of the properties of the convective clouds (D: 1, <a href="#">options?</a> ) <a href="#">meaning?</a>
fact_cldcon	1.	computation of the properties (units?) of the convective clouds (D: 0.375) <a href="#">meaning?</a>
facttemps	0.	computation of the properties (units?) of the convective clouds (D: 1.e-4) <a href="#">meaning?</a>

iflag_pdf	1	computation of the condensed water and cloud fraction from the PDF (D=0, 0: version with 'ratqs' , ≠ 0: new PDFs) <a href="#">meaning?</a>
ok_newmicro	y	computation of the optical thickness and emissivity of the clouds (D: y, n: no, y: yes)
iflag_ratqs	0	computation of the optical ( <a href="#">units?</a> ) thickness and emissivity of the clouds (D: 1) <a href="#">meaning?</a>
ratqsbas	0.005	computation of the optical ( <a href="#">units?</a> ) thickness and emissivity of the clouds (D: 0.01) <a href="#">meaning?</a>
ratqshaut	0.33	computation of the optical ( <a href="#">units?</a> ) thickness and emissivity of the clouds (D: 0.3) <a href="#">meaning?</a>
rad_froid	35	effective radius ( <a href="#">units?</a> ) for the ice clouds (D:35)
rad_chau1	12	effective radius ( <a href="#">units?</a> ) for the liquid water clouds (D: 13)
rad_chau2	11	drop size ( <a href="#">units?</a> ) of cloud water (D: 9)
new_oliq	y	selection of new oliq (D: ?, n: no, y: yes) <a href="#">meaning?</a>
<hr/> Convection		
iflag_con	30	convection scheme (D: 2, 1: LMD, 2: Tiedtke, 3: KE new physics, 30: KE IPCC)
if_ebil	0	level of output of the diagnostic of the energy conservation (D: ?)
epmax	.999	efficiency ( <a href="#">units?</a> ) of the maximum precipitation (D: .993) (see value $ep_{max}$ in section 3.2)
ok_adj_ema	n	dry convective adjustment at the beginning of the convection (D: n, n: no, y: yes)
iflag_clw	1	dry convective adjustment at the beginning of the convection (D: 0, 0: no, 1: yes)
iflag_clos	1	Closure of the convection (D: 1, 1: <a href="#">AR4</a> , 2: ALE and ALP)
iflag_mix	1	mixing rule at the entrainment (D: 1, 0: plate, 1: <a href="#">AR4</a> : <a href="#">PDF</a> )
qqa1	0.	weights of the PDFs at the flat (D: 1.)
qqa2	1.	weights of the PDFs at the bell (D: 0.)
cvl_corr	1.0	multiplicative factor of the convective precipitations in <a href="#">KE</a> (D: ?)
<hr/> planetary boundary layer		
iflag_thermals	0	<a href="#">CL</a> scheme of the thermals (D: 0, 0: dry adjustment, 1: thermal versions) <a href="#">Is suited with iflag_clos?</a>
nsplit_thermals	1	time-step splitting ( <a href="#">units?</a> ) for the thermals (D: ?)
tau_thermals	0.	time-step splitting ( <a href="#">units?</a> ) for the thermals (D: ?)
iflag_thermals_ed	0	time-step splitting ( <a href="#">units?</a> ) for the thermals (D: ?, 0: no, 1: yes)
iflag_thermals_optflux	0	time-step splitting ( <a href="#">units?</a> ) for the thermals (D: ?, 0: no, 1: yes)
iflag_pbl	1	surface layer scheme (D: 1, 1: LMD, 8: Mellor-Yamada)
ksta_ter	1.e-7	turbulent diffusion ( <a href="#">units?</a> ) (D: ?)
ksta	1.e-10	turbulent diffusion ( <a href="#">units?</a> ) (D: ?)
ok_kzmin	y	computation of Kzmin in the surface CL (D: ?, n: no, y: yes)
iflag_coupl	0	coupling with the convection (D: ?, 0: <a href="#">AR4</a> , 1: new physics)
seuil_inversion	-0.08	( <a href="#">units?</a> ) (D: ?) <a href="#">meaning?</a>
<hr/> wakes		
iflag_wake	0	activation of the wakes (D: 0, 0: no ( <a href="#">AR4</a> ), 1: new physics)
alp_offset	-0.2	( <a href="#">units?</a> ) (D: ?)

Table 8: Configuration parameters of the file 'physiq.def'. 'D' stands for 'default' value. Showed values are from the test simulation LMDZ5 - BENCH48x36x19

## 7.5 traceur.def

Configuration ASCII file for the tracers configuration

```

4      (D: ?) meaning?
14 14  H2Ov (D: ?) meaning?
10 10  H2O1 (D: ?) meaning?
10 10  RN  (D: ?) meaning?

```

Table 9: Configuration parameters of the file 'traceur.def'. 'D' stands for 'default' value. Showed values are from the test simulation LMDZ5 - BENCH48x36x19

## 7.6 orchidee.def

Configuration ASCII file for the orchidee scheme (comments in <http://forge.ipsl.jussieu.fr/orchidee/>)

STOMATE_OK_CO2	TRUE	set to TRUE if photosynthesis is to be activated (D: ?, FALSE: no, TRUE: yes)
STOMATE_OK_STOMATE	FALSE	set to TRUE if STOMATE is to be activated (D: ?, FALSE: no, TRUE: yes)
STOMATE_OK_DGVM	FALSE	set to TRUE if DGVM is to be activated (D: ?, FALSE: no, TRUE: yes)
STOMATE_WATCHOUT	FALSE	set to TRUE if you want STOMATE to read and write its start files and keep track of longer-term biometeorological variables. This is useful if OK_STOMATE is not set, but if you intend to activate STOMATE later. In that case, this run can serve as a spinup for longer-term biometeorological variables. (D: ?, FALSE: no, TRUE: yes)
<hr/>		
SECHIBA		
SECHIBA_restart_in	start_sech.nc	This is the name of the file which will be opened to extract the initial values of all prognostic values of the model. This has to be a netCDF file. Not truly COADS compliant. NONE will mean that no restart file is to be expected. (D: ?)
SECHIBA_rest_out	restart_sech.nc	This variable give the name for the restart files. The restart software within IOIPSL will add .nc if needed. (D: ?)
SECHIBA_reset_time	y	This option allows the model to override the time found in the restart file of SECHIBA with the time of the first call. That is the restart time of the GCM.(D: ?, n: no, y: yes)
OUTPUT_FILE	sechiba_out.nc	This file is going to be created by the model and will contain the output from the model. This file is a truly COADS compliant netCDF file. It will be generated by the hist software from the IOIPSL package. (D: ?)
WRITE_STEP	2592000	(D: ?)
SECHIBA_HISTLEVEL	5	Chooses the list of variables in the history file. Values between 0: nothing is written; 10: everything is written are available More details can be found on the web under documentation. (D: ?)
SECHIBA_HISTFILE2	FALSE	Chooses the list of variables in the history file. Values between 0: nothing is written; 10: everything is written are available More details can be found on the web under documentation. First level contains all ORCHIDEE outputs. (D: ?, FALSE: no, TRUE: yes)

SECHIBA_OUTPUT_FILE2	sechiba_out_2.nc	This file is going to be created by the model and will contain the output 2 from the model. (D: ?)
WRITE_STEP2	86400.0	(seconds?) (D: ?)
SECHIBA_HISTLEVEL2	1	Chooses the list of variables in the history file. Values between 0: nothing is written; 10: everything is written are available More details can be found on the web under documentation. web under documentation. First level contains all ORCHIDEE outputs. (D: ?)
<hr/>		
STOMATE		
STOMATE_OUTPUT_FILE	stomate_history.nc	This file is going to be created by the model and will contain the output from the model. This file is a truly COADS compliant netCDF file. It will be generated by the hist software from the IOIPSL package. (D: ?)
STOMATE_HIST_DT	10.	Time step (days) of the STOMATE history file (D: ?)
STOMATE_HISTLEVEL	0	Chooses the list of variables in the history file. Values between 0: nothing is written; 10: everything is written are available More details can be found on the web under documentation. (D: ?)
SECHIBA_DAY	0.0	This is the time spent simulating the current day (in days). This variable is prognostic as it will trigger all the computations which are only done once a day. (D: ?)
SECHIBA_ZCANOP	0.5	The temperature at this soil depth (in meters) is used to determine the LAI when STOMATE is not activated. (D: ?)
DT_SLOW	86400.	Time step (in seconds) of regular update of vegetation cover, LAI etc. This is also the time step of STOMATE. (D: ?)
IMPOSE_VEG	FALSE	This flag allows the user to impose a vegetation distribution and its characteristics. It is especially interesting for 0D simulations. On the globe it does not make too much sense as it imposes the same vegetation everywhere
VEGETATION_FILE	carteveg5km.nc	The name of the file to be opened to read a vegetation map (in pft) is to be given here. (D: ?, carteveg5km.nc: , pft_new.nc: )
DIFFUCO_LEAF_CI	233.	The initial value of leaf_ci if its value is not found in the restart file. This should only be used if the model is started without a restart file. (D: ?)
CONDVEG_SNOWA	default (1.E+20?)	This option allows the user to impose a snow albedo. Default behaviour is to use the model of snow albedo developed by [CT94]. (D: ?)
IMPOSE_AZE	FALSE	This flag allows the user to impose the surface parameters (Albedo Roughness and Emissivity). It is specially interesting for 0D simulations. On the globe it does not make too much sense as it imposes the same vegetation everywhere (D: ?, FALSE: no, TRUE: yes)

SOILALB_FILE	soils_param.nc	The name of the file to be opened to read the soil types from which we derive then the bare soil albedos. This file is 1x1 deg and based on the soil colors defined by Wilson and Henderson-Seller. (D: ?)
SOILTYPE_FILE	soils_param.nc	(D: ?)
ENERBIL_TSURF	280.	(K?) (D: ?)
hydrology		
HYDROL_SNOW	0.0	The initial value of snow mass if its value is not found in the restart file. This should only be used if the model is started without a restart file. (D: ?)
HYDROL_SNOWAGE	0.0	The initial value of snow age if its value is not found in the restart file. This should only be used if the model is started without a restart file. (D: ?)
HYDROL_SNOWICE	0.0	(D: ?)
HYDROL_SNOWICEAGE	0.0	(D: ?)
HYDROL_HDRY	1.0	(D: ?)
HYDROL_HUMR	1.0	The initial value of soil moisture stress if its value is not found in the restart file. This should only be used if the model is started without a restart file. (D: ?)
HYDROL_BQSB	default (999999.?)	The initial value (in $kgm^{-2}$ ) of deep soil moisture if its value is not found in the restart file. This should only be used if the model is started without a restart file. Default behaviour is a saturated soil. (D: ?)
HYDROL_GQSB	0.0	The initial value (in $kgm^{-2}$ ) of upper soil moisture if its value is not found in the restart file. This should only be used if the model is started without a restart file. (D: ?)
HYDROL_DSG	0.0	The initial value (in meters) of upper reservoir depth if its value is not found in the restart file. This should only be used if the model is started without a restart file. (D: ?)
HYDROL_DSP	default (999999.?)	The initial value (in meters) of dry soil above upper reservoir if its value is not found in the restart file. This should only be used if the model is started without a restart file. The default behaviour is to compute it from the variables above. Should be OK most of the time (D: ?)
HYDROL_QSV	0.0	The initial value (in $kgm^{-2}$ ) of moisture on canopy if its value is not found in the restart file. This should only be used if the model is started without a restart file. (D: ?)
HYDROL_OK_HDIFF	n	If TRUE, then water can diffuse horizontally between the PFTs' water reservoirs. (D: ?, n: no, y: yes)
HYDROL_TAU_HDIFF	1800.	Defines (in seconds) how fast diffusion occurs horizontally between the individual PFTs' water reservoirs. If infinite, no diffusion. (D: ?)
THERMOSOIL_TPRO	280.	(K?) (D: ?)



RIVER_ROUTING	y	This flag allows the user to decide if the runoff and drainage should be routed to the ocean and to downstream grid boxes. (D: ?, n: no, y: yes)
ROUTING_FILE	routing.nc	The file provided here should allow the routing module to read the high resolution grid of basins and the flow direction from one mesh to the other.(D: ?)
LAI_MAP	y	It is possible to read a 12 month LAI map which will then be interpolated to daily values as needed. (D: ?, n: no, y: yes)
LAI_FILE	lai2D.nc	The name of the file to be opened to read the LAI map is to be given here (in combination with LAI_MAP=n). Usually SECHIBA runs with a 5kmx5km map which is derived from a Nicolas VIOVY one. (D: ?)
SECHIBA_QSINT	0.02	Transforms leaf area index into size (in meters) of interception reservoir for slowproc_derivvar or stomate (D: ?)
ALB_BARE_MODEL	FALSE	If TRUE, the model for bare soil albedo is the old formulation. Then it depend on the soil dry or wetness. If FALSE, it is the new computation that is taken, it is the mean of soil albedo. (D: ?, FALSE: no, TRUE: yes)
PERCENT_THROUGHFALL_PFT	30., 30., 30., 30., 30., 30., 30., 30., 30., 30., 30., 30., 30.	During one rainfall event, PERCENT_THROUGHFALL_PFT (in %) of the incident rainfall will get directly to the ground without being intercepted, for each PFT. (D: ?)
RVEG_PFT	.5, .5, .5, .5, .5, .5, .5, .5, .5, .5, .5, .5, .5	Artificial parameter to increase or decrease canopy resistance. This parameter is set by PFT. (D: ?)
CDRAG_FROM_GCM	.TRUE.	Set to .TRUE. if you want q_cdrag coming from GCM (if q_cdrag on initialization is non zero). Keep cdrag coefficient from gcm for latent and sensible heat fluxes.(D: ?)
LAND_USE	y	pft values are needed, max time axis is 293
VEGET_YEAR	0	First year for landuse vegetation (2D map by pft). If VEGET_YEAR is set to 0, this means there is no time axis.
VEGET_UPDATE	1Y	The veget datas (in years) will be update each this time step

Are other options for the input files? Format of files?  
What about all the other parameters?

---

Table 10: Configuration parameters of the file 'orchidee.def' taken from <http://forge.ipsl.jussieu.fr/orchidee/wiki/Documentation/OrchideeParameters>. 'D' stands for 'default' value. Showed values are from the test simulation LMDZ5 - BENCH48x36x19

## References

[Bat67] G. K. Batchelor. An Introduction to Fluid Dynamics. Cambridge University Press, 1967.



- [BE01] S. Bony and K. A. Emanuel. A parameterization of the cloudiness associated with cumulus convection; evaluation using toga coare data. *J. Atmos. Sci.*, 58:3158–3183, 2001.
- [BL95] O. Boucher and U. Lohmann. The sulfate-ccn-cloud albedo effect. *Tellus B*, 47(3):281–300, 1995.
- [Cho77] E. Choissnel. Un modèle agrométéorologique opérationnel de bilan hydrique utilisant des données climatiques. *Les besoins en eau des cultures. Proc. Conférence internationale CIID. Paris, 1977.*
- [CT94] S. Chalita and H. Treut. The albedo of temperate and boreal forest and the northern hemisphere climate: a sensitivity experiment using the lmd gcm. *Climate Dynamics*, 10(4-5):231–240, 1994.
- [Dea66] J. W. Deardorff. The counter-gradient heat flux in the lower atmosphere and in the laboratory. *J. Atmos. Sci.*, 23:503–506, 1966.
- [DFD+13] J. L. Dufresne, M. A. Foujols, S. Denvil, A. Caubel, O. Marti, O. Aumont, Y. Balkanski, S. Bekki, H. Bellenger, R. Benshila, S. Bony, L. Bopp, P. Braconnot, P. Brockmann, P. Cadule, F. Cheruy, F. Codron, A. Cozic, D. Cugnet, N. Noblet, J. P. Duvel, C. Ethé, L. Fairhead, T. Fichefet, S. Flavoni, P. Friedlingstein, J. Y. Grandpeix, L. Guez, E. Guilyardi, D. Hauglustaine, F. Hourdin, A. Idelkadi, J. Ghattas, S. Joussaume, M. Kageyama, G. Krinner, S. Labetoulle, A. Lahellec, M. P. Lefebvre, F. Lefevre, C. Levy, Z. X. Li, J. Lloyd, F. Lott, G. Madec, M. Mancip, M. Marchand, S. Masson, Y. Meurdesoif, J. Mignot, I. Musat, S. Parouty, J. Polcher, C. Rio, M. Schulz, D. Swingedouw, S. Szopa, C. Talandier, P. Terray, N. Viovy, and N. Vuichard. Climate change projections using the ipsl-cm5 earth system model: from cmip3 to cmip5. *Clim. Dyn.*, 40(9-10):2123–2165, 2013.
- [DLP93] N. I. Ducoudré, K. Laval, and A. Perrier. Sechiba, a new set of parameterizations of the hydrologic exchanges at the land-atmosphere interface within the lmd atmospheric general circulation model. *J. Climate*, 6:248–273, 1993.
- [dRP98] P. de Rosnay and J. J. Polcher. Modelling root water uptake in a complex land surface scheme coupled to a gcm. *Hydrol. Earth Syst. Sci.*, 2(2/3):239–255, 1998.
- [Ema91] K. A. Emanuel. A scheme for representing cumulus convection in large-scale models. *J. Atmos. Sci.*, 48:2313–2329, 1991.
- [Ema93] K. A. Emanuel. A cumulus representation based on the episodic mixing model: the importance of mixing and microphysics in predicting humidity. *AMS Meteorol. Monogr.*, 24:185–192, 1993.
- [EuR99] K. A. Emanuel and M. Živković Rothman. Development and evaluation of a convection scheme for use in climate models. *J. Atmos. Sci.*, 56:1766–1782, 1999.
- [FB80] Y. Fouquart and B. Bonnel. Computations of solar heating of the earth’s atmosphere: A new parameterization. *Beitr. Phys. Atmos.*, 53:35–62, 1980.
- [Fou88] Y. Fouquart. Radiative transfer in climate models. In M.E. Schlesinger, editor, *Physically-Based Modelling and Simulation of Climate and Climatic Change*, volume 243 of *NATO ASI Series*, pages 223–283. Springer Netherlands, 1988.
- [Gel77] J. F. Geleyn. A comprehensive radiation scheme designed for fast computation. *Res. Dep. Eur. Cent. for Medium Range Weather Forecasts, Reading, England, Internal Rep. 8.:36*, 1977.
- [GL09] J. Y. Grandpeix and J. P. Lafore. A density current parameterization coupled with emanuels convection scheme. part i: The models. *J. Atmos. Sci.*, 67:881–897, 2009.
- [GLC09] J. Y. Grandpeix, J. P. Lafore, and F. Cheruy. A density current parameterization coupled with emanuels convection scheme. part ii: 1d simulations. *J. Atmos. Sci.*, 67:898–922, 2009.
- [GPT04] J. Y. Grandpeix, V. Phillips, and R. Tailleux. Improved mixing representation in emanuel’s convection scheme. *Q. J. R. Meteorol. Soc.*, 130(604):3207–3222, 2004.
- [Gur65] M. I. Gurevich. *Theory Of Jets In Ideal Fluids*. Academic Press (Translated From The Russian Edition), 1965.

- [HCM02] F. Hourdin, F. Couvreux, and L. Menut. Parameterization of the dry convective boundary layer based on a mass flux representation of thermals. *J. Atmos. Sci.*, 59:1105–1123, 2002.
- [HD90] A. J. Heymsfield and L. J. Donner. A scheme for parameterizing ice-cloud water content in general circulation models. *J. Atmos. Sci.*, 47:1865–1877, 1990.
- [HFC+13] F. Hourdin, M. A. Foujols, F. Codron, V. Guemas, J. L. Dufresne, S. Bony, S. Denvil, L. Guez, F. Lott, J. Ghattas, P. Braconnot, O. Marti, Y. Meurdesoif, and L. Bopp. Impact of the lmdz atmospheric grid configuration on the climate and sensitivity of the ipsl-cm5a coupled model. *Climate Dynamics*, 40(9-10):2167–2192, 2013.
- [HGR+13] F. Hourdin, J. Y. Grandpeix, C. Rio, S. Bony, A. Jam, F. Cheruy, N. Rochetin, L. Fairhead, A. Idelkadi, I. Musat, J. L. Dufresne, A. Lahellec, M. P. Lefebvre, and R. Roehrig. Lmdz5b: the atmospheric component of the ipsl climate model with revisited parameterizations for clouds and convection. *Clim. Dyn.*, 40(9-10):2193–2222, 2013.
- [Jar76] P. G. Jarvis. The interpretation of the variations in leaf water potential and stomatal conductance found in canopies in the field. *Phil. Trans. R. Soc. Lond. B*, 273:593–610, 1976.
- [JHRC11] A. Jam, F. Hourdin, C. Rio, and F. Couvreux. Resolved versus parameterized boundary-layer plumes. part iii: a diagnostic boundary-layer cloud parameterization derived from large eddy simulations. submitted to *BLM*, 2011.
- [Kir77] G. Kirchoff. Vorlesungen über mathematische physik. Mechanik / von Dr.Gustav Robert Kirchhoff. Leipzig, 1877.
- [KVdND+05] G. Krinner, N. Viovy, N. de Noblet-Ducoudré, J. Ogée, J. Polcher, P. Friedlingstein, P. Ciais, S. Sitch, and I. C. Prentice. A dynamic global vegetation model for studies of the coupled atmosphere-biosphere system. *Global Biogeochem. Cy.*, 19(1):n/a–n/a, 2005.
- [Lan61] L. Landweber. Motion of immersed and floating bodies. McGraw-Hill (1st ed.), 1961.
- [LLLF80] T. Lohammar, S. Larsson, S. Linder, and S. O. Falk. Fast: Simulation models of gaseous exchange in scots pine. *Ecological Bulletins*, 32:505–523, 1980.
- [LM97] F. Lott and M. J. Miller. A new subgrid-scale orographic drag parametrization: Its formulation and testing. *Q. J. R. Meteorolo. Soc.*, 123(537):101–127, 1997.
- [Mat83a] E. Matthews. Global vegetation and land use: New high-resolution data bases for climate studies. *J. Climate Appl. Meteor.*, 22:474–487, 1983.
- [Mat83b] E. Matthews. Prescription of land-surface boundary conditions in giss gcm ii: A simple method based on high-resolution vegetation data bases. *Tech. Memo. NASA*, 86096:20, 1983.
- [Mat84] E. Matthews. Vegetation, land-use and seasonal albedo data sets: documentation of archived data tape. *Tech. Memo. NASA*, 86107:12, 1984.
- [MF85] J. J. Morcrette and Y. Fouquart. On systematic errors in parametrized calculations of longwave radiation transfer. *Q. J. of R. Meteorol. Soc.*, 111(469):691–708, 1985.
- [MF86] J.J. Morcrette and Y. Fouquart. The overlapping of cloud layers in shortwave radiation parameterizations. *J. Atmos. Sci.*, 43:321–328, 1986.
- [MFS+72] R. A. McClatchey, R. W. Fenn, J. E. A. Selby, F. E. Volz, and J. S. Garing. Optical Properties of the Atmosphere. Environ. Res. Pap. (3rd Ed.) Air Force Cambridge Research Labs Hanscom Afb MA, 1972.
- [Mon63] J. L. Monteith. Gas exchange in plant communities. Academic Press, New York, USA, 1963.
- [Mor90] J.J. Morcrette. Impact of changes to the radiation transfer parameterizations plus cloud optical. properties in the ecmwf model. *Mon. Wea. Rev.*, 118:847–873, 1990.

- [Mor91] J. J. Morcrette. Radiation and cloud radiative properties in the european centre for medium range weather forecasts forecasting system. J. Geophys. Research: Atmospheres, 96(D5):9121–9132, 1991.
- [MSF86] J. J. Morcrette, L. Smith, and Y. Fouquart. Pressure and temperature dependence of the absorption in longwave radiation parametrizations. Beiträge zur Physik der Atmosphäre, 59:455–469, 1986.
- [MY74] G. L. Mellor and T. Yamada. A hierarchy of turbulence closure models for planetary boundary layers. J. Atmos. Sci., 31:1791–1806, 1974.
- [Phi84] D. S. Phillips. Analytical surface pressure and drag for linear hydrostatic flow over three-dimensional elliptical mountains. J. Atmos. Sci., 41:1073–1084, 1984.
- [RH08] C. Rio and F. Hourdin. A thermal plume model for the convective boundary layer: Representation of cumulus clouds. J. Atmos. Sci., 65:407–425, 2008.
- [RHCJ10] C. Rio, F. Hourdin, F. Couvreux, and A. Jam. Resolved versus parametrized boundary-layer plumes. part ii: Continuous formulations of mixing rates for mass-flux schemes. Boundary-Layer Meteorology, 135(3):469–483, 2010.
- [SC81] N. A. Scott and A. Chédin. A fast line-by-line method for atmospheric absorption computations - the automatized atmospheric absorption atlas. J. of Appl. Meteor., 20:802–812, 1981.
- [Shu88] W. J. Shuttleworth. Evaporation from amazonian rainforest. Proc. R. Soc. Lond. B, 233:321–346, 1988.
- [SK91] B. Saugier and N. Katerji. Some plant factors controlling evapotranspiration. Agric. Forest Meteor., 54(2-4):263 – 277, 1991.
- [SSP+03] S. Sitch, B. Smith, I. C. Prentice, A. Arneth, A. Bondeau, W. Cramer, J. O. Kaplan, S. Levis, W. Lucht, M. T. Sykes, K. Thonicke, and S. Venevsky. Evaluation of ecosystem dynamics, plant geography and terrestrial carbon cycling in the lpj dynamic global vegetation model. Global Change Biol., 9(2):161–185, 2003.
- [SSR+89] N. Sato, P. J. Sellers, D. A. Randall, E. K. Schneider, J. Shukla, J. L. Kinter, Y. T. Hou, and E. Albertazzi. Effects of implementing the simple biosphere model in a general circulation model. J. Atmos. Sci., 46:2757–2782, 1989.
- [Ste78] G. L. Stephens. Radiation profiles in extended water clouds. ii: Parameterization schemes. J. Atmos. Sci., 35:2123–2132, 1978.
- [Stu88] R. B. Stull. An introduction to boundary layer meteorology. Kluwer Academic Publishers, 1988.
- [Sun78] H. Sundqvist. A parameterization scheme for non-convective condensation including prediction of cloud water content. Q. J. R. Meteorol. Soc., 104(441):677–690, 1978.
- [Sun88] H. Sundqvist. Parameterization of condensation and associated clouds in models for weather prediction and general circulation simulation. In M.E. Schlesinger, editor, Physically-Based Modelling and Simulation of Climate and Climatic Change, volume 243 of NATO ASI Series, pages 433–461. Springer Netherlands, 1988.
- [Vig53] E. Vigroux. Contribution à l’étude expérimentale de l’absorption de l’ozone. Ann. Phys., 8:709, 1953.
- [WMO84] WMO. The intercomparison of radiation codes in climate models (icrcm), longwave, clear-sky calculations. World Climate Programme, Geneva, Switzerland, Rep. WCP-93:37, 1984.
- [Yam83] T. Yamada. Simulations of nocturnal drainage flows by a  $q^2l$  turbulence closure model. J. Atmos. Sci., 40:91–106, 1983.
- [ZK97] C. S. Zender and J. T. Kiehl. Sensitivity of climate simulations to radiative effects of tropical anvil structure. J. Geophys. Res.: Atmospheres, 102(D20):23793–23803, 1997.